JACS
JOURNAL OF THE AMERICAN CHEMICAL SOCIETY
Article
pubs.acs.org/JACS

Tin-Free Direct C–H Arylation Polymerization for High Photovoltaic Efficiency Conjugated Copolymers

Alexander S. Dudnik,[†,§] Thomas J. Aldrich,[†,§] Nicholas D. Eastham,[†,‡] Robert P. H. Chang,[*,‡] Antonio Facchetti,[*,‡,⊥] and Tobin J. Marks[*,†,‡]

[†]Department of Chemistry and the Materials Research Center, Northwestern University, 2145 Sheridan Road, Evanston, Illinois 60208, United States

[‡]Department of Materials Science and Engineering and Argonne Northwestern Solar Energy Research Center (ANSER), Northwestern University, 2145 Sheridan Road, Evanston, Illinois 60208, United States

[⊥]Polyera Corporation, 8045 Lamon Avenue, Skokie, Illinois 60077, United States

Supporting Information

ABSTRACT: A new and highly regioselective direct C–H arylation polymerization (DARP) methodology enables the reproducible and sustainable synthesis of high-performance π-conjugated photovoltaic copolymers. Unlike traditional Stille polycondensation methods for producing photovoltaic copolymers, this DARP protocol eliminates the need for environmentally harmful, toxic organotin compounds. This DARP protocol employs low loadings of commercially available catalyst components, $Pd_2(dba)_3{\cdot}CHCl_3$ (0.5 mol%) and P(2-MeOPh)$_3$ (2 mol%), sterically tuned carboxylic acid additives, and an environmentally friendly solvent, 2-methyltetrahydrofuran. Using this DARP protocol, several representative copolymers are synthesized in excellent yields and high molecular masses. The DARP-derived copolymers are benchmarked versus Stille-derived counterparts by close comparison of optical, NMR spectroscopic, and electrochemical properties, all of which indicate great chemical similarity and no significant detectable structural defects in the DARP copolymers. The DARP- and Stille-derived copolymer and fullerene blend microstructural properties and morphologies are characterized with AFM, TEM, and XRD and are found to be virtually indistinguishable. Likewise, the charge generation, recombination, and transport characteristics of the fullerene blend films are found to be identical. For the first time, polymer solar cells fabricated using DARP-derived copolymers exhibit solar cell performances rivalling or exceeding those achieved with Stille-derived materials. For the DARP copolymer **PBDTT-FTTE**, the power conversion efficiency of 8.4% is a record for a DARP copolymer.

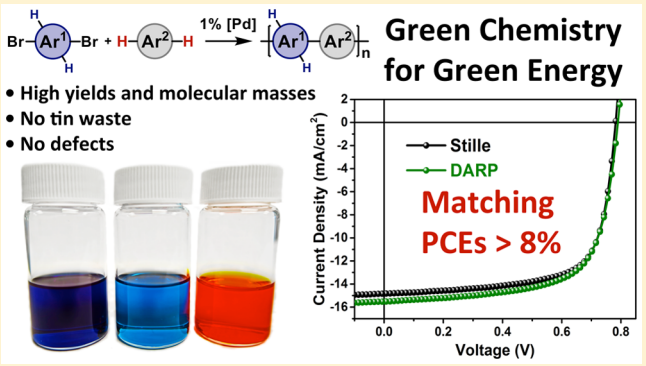

INTRODUCTION

π-Conjugated donor–acceptor copolymers consisting of alternating in-chain electron-rich and electron-deficient subunits are promising solution-processable photoactive layer semiconductors for polymer solar cells (PSCs).[1−5] Power conversion efficiencies (PCEs) >11% have been recently achieved in bulk-heterojunction (BHJ) PSCs utilizing this donor–acceptor copolymer design strategy, which demonstrates the potential of this technology for inexpensive and sustainable energy generation.[6] To date, π-conjugated in-chain donor–acceptor copolymers have primarily been prepared by Pd-catalyzed Stille polycondensation reactions involving toxic stannylated comonomers (Figure 1a),[6,7] which presents a major obstacle in their large-scale production. Specifically, synthesizing the stannylated comonomers requires toxic tin reagents, and the subsequent Stille reactions generate stoichiometric quantities of toxic organotin waste, the large-scale disposal of which is costly and raises serious environmental concerns.[8,9] Considering the great potential and rapid advances in PSCs, there is urgent need to develop sustainable, atom-efficient, and environmentally benign polymerization methods for the large-scale synthesis of these high-performance copolymers.

Direct C–H arylation polymerization (DARP) is an emerging sustainable polymerization approach (Figure 1a), and promising studies have yielded π-conjugated copolymers with appreciable number-average and weight-average molecular masses (M_ns and M_ws, respectively),[10−13] in addition to charge transport properties similar to those of Stille-derived copolymers.[14−17] Note that DARP reaction byproducts are benign and one of the comonomers is unfunctionalized (C–H terminated), affording overall more concise and atom-economical synthetic sequences.[10,11,18] The cost savings of DARP processes relative

Received: September 23, 2016
Published: November 9, 2016

DOI: 10.1021/jacs.6b10023
J. Am. Chem. Soc. 2016, 138, 15699−15709

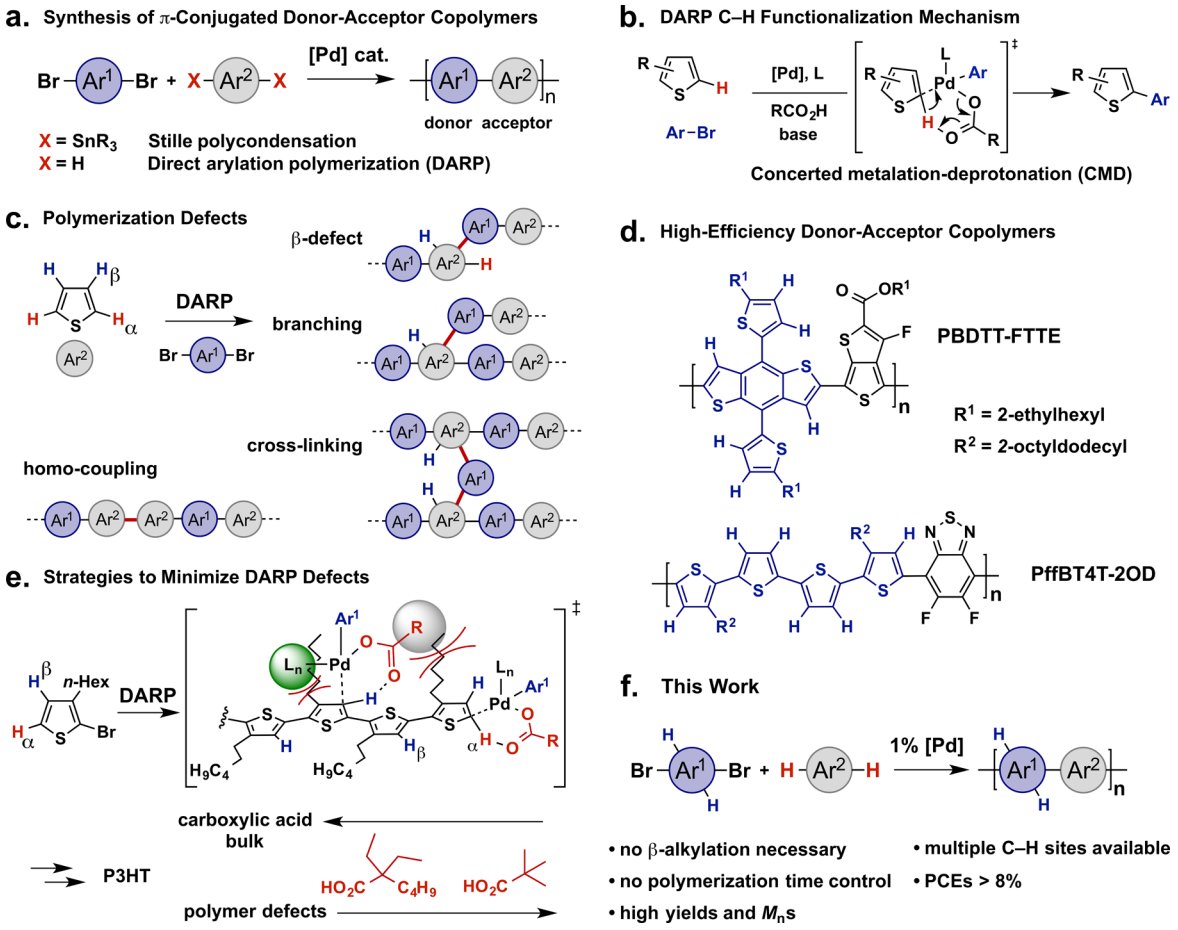

Figure 1. Synthesis of semiconducting π-conjugated polymers. (a) Comparison of traditional Stille cross-coupling polycondensation and direct arylation polymerization (DARP) for the synthesis of π-conjugated donor−acceptor copolymers. The Stille process generates 1.0 equiv of toxic R_3SnBr byproduct for each carbon−carbon bond created. (b) Concerted metalation−deprotonation (CMD) mechanism for C−H functionalization of thiophene-based comonomers in the presence of a carboxylic acid additive. (c) Defect types that can occur in thiophene-based copolymers synthesized via DARP. (d) Examples of semiconducting copolymers with high photovoltaic efficiency containing thiophene units with multiple reactive C−H bonds. (e) Example of a strategy to minimize polymer defects in DARP-derived homopolymers. Bulkier carboxylate ligands suppress detrimental β-C−H functionalization of the polymer backbone. (f) The present DARP approach to donor−acceptor copolymers.

to Stille polycondensations was recently estimated to be as high as 35%, making DARP remarkably attractive.[14]

The key mechanistic step in DARP involves a Pd-catalyzed regioselective aryl C−H bond functionalization that proceeds via a concerted metalation−deprotonation (CMD) process in the presence of a carboxylic acid additive (Figure 1b).[19−21] Note however that for monomers having multiple reactive C−H bonds, as in β-unfunctionalized (oligo)thiophenes, high regioselectivity for the α-position is essential for useful DARP-syntheses of semiconducting polymers.[22] Importantly, unlike C−H functionalization reactions of small molecules where undesired byproducts can often be easily separated, most DARP defects (e.g., β-defects, branching, cross-linking, homocoupling) remain embedded in the polymer structure (Figure 1c)[22,23] and severely degrade charge transport/photovoltaic performance.[22,24−27] Furthermore, achieving high polymerization conversions (>95%) and thus high polymer M_ns is often essential for optimal optoelectronic device performance.[28−31] As a DARP reaction progresses and longer polymer chains are generated, the ratio of "desired" target C−H end groups decreases rapidly relative to the "undesired" polymer backbone aryl C−H bonds.[11] Thus, exceptional C−H functionalization regioselectivities (>100−200:1) are critical to suppress polymer branching defects. Previous approaches to minimize defects in DARP-derived copolymers have included functionalizing monomers (e.g., thiophene β-position alkylation) to eliminate "undesired" C−H sites,[16] employing directing groups,[11,12] polymer-specific polymerization reaction time tuning,[32] and using monomers with a single reactive C−H bond type.[10,11,22] However, the generality of these strategies is typically limited, especially considering that the overwhelming majority of high-performance π-conjugated copolymers contain abundant aryl C−H bonds (Figure 1d).[6,33] Furthermore, monomer β-functionalization often induces polymer backbone distortion which can unpredictably and often detrimentally impact performance.[34] In view of these challenges, it is not surprising that the maximum reported photovoltaic performance of DARP-synthesized copolymers remains modest, with PCEs mostly below 6%.[34−50] Indeed, our attempts to prepare a known high-performance donor−acceptor copolymer using established DARP protocols were unsuccessful (*vide infra*).

Pioneering studies by Thompson[51] and Leclerc[52] established that sterically demanding carboxylic acid additives, such as neodecanoic acid suppress the formation of β- and branching defects in DARP reactions of bifunctional AB-type monomers. Steric repulsion between the Pd carboxylate ligand and the

DOI: 10.1021/jacs.6b10023
J. Am. Chem. Soc. 2016, 138, 15699−15709

solubilizing alkyl side chains along the polymer backbone is thought to diminish the reactivity of "undesired" β- versus the more sterically accessible α-C−H sites (Figure 1e).[22,51] While this approach can provide defect-free DARP homopolymers such as poly(3-hexylthiophene) (**P3HT**) and related polyalkylthiophenes with thermal and optical properties matching those of Stille-derived materials, no general correlation with photovoltaic efficiencies has been established for a broad range of polymers.[50−52] To the best of our knowledge, the DARP of two distinctly different comonomers (AA/BB-type) with multiple aryl C−H bonds and without β-C−H protecting groups has not yet afforded highly efficient PSCs and remains an unfulfilled challenge.

Here we report a general and efficient Pd-catalyzed DARP process employing a new bulky carboxylic acid additive for preparing five known high-performance donor−acceptor semiconducting copolymers (Figure 1f). We show here that these DARP copolymers display physical and chemical properties as well as photovoltaic performances that equal or exceed those of Stille-derived references. The DARP copolymers are obtained in high yields, with M_ns comparable to their Stille counterparts, and without detectable structural defects, despite the abundance of "undesired" reactive C−H sites along the copolymer backbones. Note that this process employs a low catalyst loading and an environmentally friendly solvent, thereby increasing its practicality.[8,12] An in-depth investigation of the bulk charge transport (SCLC), charge generation/recombination (light intensity studies), and thin-film morphological properties (AFM, TEM, and XRD) of the DARP- and Stille-derived BHJ blends is performed using a battery of physical methods. The results evidence impressive similarities between the Stille- and DARP-derived copolymers and the absence of detrimental structural defects in the latter. Finally, we demonstrate PSC efficiencies exceeding 8%, a record for DARP copolymers.

RESULTS AND DISCUSSION

Reaction Design and Optimization. For DARP to supplant Stille polycondensation, it must produce copolymers with PSC performances matching or exceeding those of Stille-derived copolymers and be applicable to many high-performance materials. While there are a few examples of DARP copolymers having PCEs equaling those of Stille-derived materials, none include high-performance copolymers, and the resulting PCEs are around or below 5%.[39,50,53] Thus, we initially explored the DARP synthesis of the copolymer poly{4,8-bis(5-(2-ethylhexyl)thiophen-2-yl)benzo[1,2-*b*:4,5-*b*′]dithiophene-2,6-diyl-*alt*-(4-(2-ethylhexyl)-3-fluorothieno-[3,4-*b*]thiophene-2-carboxylate-2,6-diyl)} (**PBDTT-FTTE**; Figure 1d), a commercially available "blockbuster" with broad utility in multiple high-performance PSCs when blended with fullerenes,[33,54−58] n-type copolymers,[59,60] and non-fullerene small-molecule acceptors,[61−65] as well as in tandem[66−69] and ternary[70−72] photovoltaics.

Regarding reaction optimization, significant challenges to DARP methodology lie in identifying reaction conditions affording *both* high regioselectivity and high reactivity, in a way that affords copolymers with minimal defects and high molecular masses. Furthermore, DARP conditions should preferably incorporate low catalyst loadings, commercially available catalyst components, and "green" solvents, as well as provide high polymer yields with minimal required purification.[73,74] Inspired by the Ozawa reports and following the above criteria, a large screen of reaction conditions was explored for the DARP of comonomers **1** and **2** (Table 1; Tables S1, S3, S5, and S7 in the Supporting Information (SI)). The product **PBDTT-FTTE** copolymers were characterized by high-temperature gel permeation chromatography (GPC) and optical absorption spectroscopy. Findings highlighting important trends are summarized in Table 1, with data for the reference Stille-derived copolymer designated batch 1.

Based on the combined optical and PSC performance data for the DARP **PBDTT-FTTE** samples, we conclude that the optical absorption properties correlate with PSC performance (see Section 4 in the SI). Specifically, a stronger degree of copolymer aggregation/ordering in solution, assayed by the peak intensity ratio ($A_{0\text{-}0}/A_{0\text{-}1}$) between the absorbance maximum and absorbance shoulder[75] generally correlates with higher PCEs.[28] The DARP **PBDTT-FTTE** batch best exemplifying this solution aggregation was obtained from polymerization conditions that employ 1% Pd catalyst and the sterically demanding 2,2-diethylhexanoic acid (DEHA) additive (Table 1, batch 2). This copolymer batch was isolated in excellent 98% yield with M_n = 25 kg/mol and dispersity ($Đ$) = 2.2, closely matching the reference Stille copolymer and other literature reports.[54−56] The additive DEHA is an isomerically pure tertiary carboxylic acid and is more bulky than the previously employed neodecanoic acid,[50−52] which is a mixture of several less encumbered $C_9H_{19}CO_2H$ isomers.[22] The DARP solvent, 2-methyltetrahydrofuran (2MeTHF), is a "green" solvent derived from renewable resources,[76] which enables facile C−H functionalization for rapid, high-conversion polymerization. Furthermore, its high boiling point enhances polymer solubility and enables a wider reaction temperature range. Increasing the Pd catalyst loading from 1 to 2% leads to a marginally higher M_n at the expense of a larger dispersity, which ultimately translates into a slightly lower quality material as judged by optical and photovoltaic properties, and in line with recent reports where device performance is not necessarily improved by increasing polymer M_n (Table 1, batch 3; Table S2 in SI).[29,31,77] Overall there is a very interesting dependence of copolymer M_n and M_w on the catalyst loading (Figure S1 in SI). Increasing the catalyst loading from 0.5 to 2% results in **PBDTT-FTTE** M_n and M_w increases from 14 to 28 kg/mol and from 35 to 80 kg/mol, respectively. This is consistent with increasing functional group conversion at higher catalyst loadings; however, both M_n and M_w fall at the even higher catalyst loadings of 4% and 8%. This result is attributed to detrimental reaction pathways, such as catalytic debromination of **1**, which likely depend on catalyst loading.[14,40,52,78] The sterically demanding DEHA additive is essential for obtaining high-M_n **PBDTT-FTTE**. The more traditionally employed, but less bulky, pivalic acid (PivOH) affords copolymers of notably lower M_n = 16 kg/mol and higher dispersity, resulting in poor optical and photovoltaic properties (Table 1, batch 4; see also batches 14 and 15 in Table S5 in SI). As discussed above, bulky carboxylic acid additives are thought to suppress β-defect formation in DARP homopolymers,[51,52] and we envision that the same benefit extends to the present system, especially considering the high reaction temperatures. DARP reaction concentration effects were investigated at high (75 mM) and low (37.5 mM) concentrations, spanning the range of typical **PBDTT-FTTE** Stille polymerization reaction concentrations (Table S3 in SI).[54−56] Lower concentrations result in lower M_ns, likely reflecting slower reaction kinetics in more dilute solutions. At higher concentrations, M_n is almost invariant,

DOI: 10.1021/jacs.6b10023
J. Am. Chem. Soc. 2016, 138, 15699−15709

Table 1. Optimization of the Direct Arylation Polymerization for PBDTT-FTTE[a]

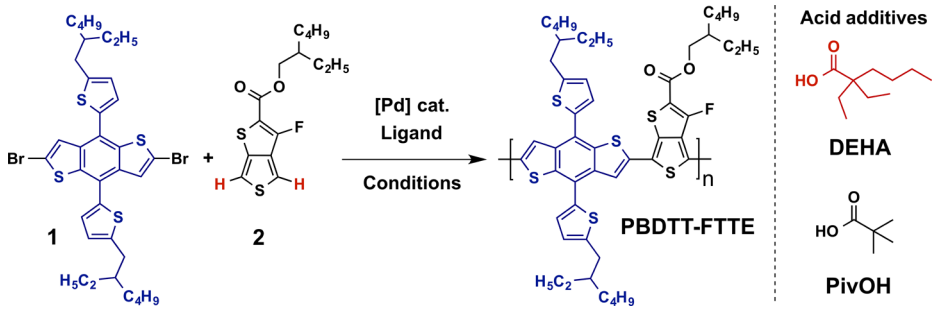

batch	Pd load (mol%)	solvent	conc (mM)	acid	yield (%)	M_n[b] (kg/mol)	$Đ$	λ_{max}[c] (nm)	$A_{0\text{-}0}/A_{0\text{-}1}$[d]	PCE[e] (%)
1[f]						24.8	2.19	640,[g] 704	1.29	8.24
2	**1**	**2MeTHF**	**50**	**DEHA**	**98**	**24.5**	**2.18**	**641,[g] 709**	**1.40**	**8.19**
3	2	2MeTHF	50	DEHA	96	28.1	2.83	641,[g] 709	1.39	7.24
4	2	2MeTHF	50	PivOH	94	16.0	2.63	639,[g] 705	1.23	6.54
5[h]	5	toluene	50	PivOH	50	5.4	1.76	618		3.85
6[h]	5	toluene	50	PivOH	49	5.0	1.61	607		2.59
7[h]	4	THF	200		26	4.8	1.38	605		1.89
8[h]	10	THF	100	PivOH	97	16.1	1.85	636[g], 706	1.18	4.88

[a]DARP reaction conditions: **1** (0.1 mmol), **2** (0.1 mmol), $Pd_2(dba)_3{\cdot}CHCl_3$ (0.5−1 mol%), P(2-MeOPh)$_3$ (2−4 mol%, Pd:ligand = 1:2), Cs_2CO_3 (3 equiv), acid additive (25 mol%) in solvent listed at concentration listed at 85 °C for 24 h. Yields are isolated yields after purification via Soxhlet extraction. [b]Determined by GPC at 150 °C in 1,2,4-trichlorobenzene. [c]Solution absorption spectra (0.013 mg/mL in 1,2-dichlorobenzene). When two numbers are provided, the second corresponds to absorption peak maximum or vibronic $A_{0\text{-}0}$ band. [d]Absorbance maximum peak intensity relative to absorbance shoulder. [e]Average power conversion efficiencies (PCEs) for solar cells based on copolymer:$PC_{71}BM$ blends. For full solar cell performance characterization results see below and Sections 4 and 7 in the SI. [f]Reference copolymer made via Stille polycondensation. [g]Absorbance shoulder or vibronic $A_{0\text{-}1}$ band. [h]Performed according to reported DARP procedures. For complete reaction conditions see Table S9 in SI.

Table 2. Substrate Scope for the Direct Arylation Polymerization (DARP)[a]

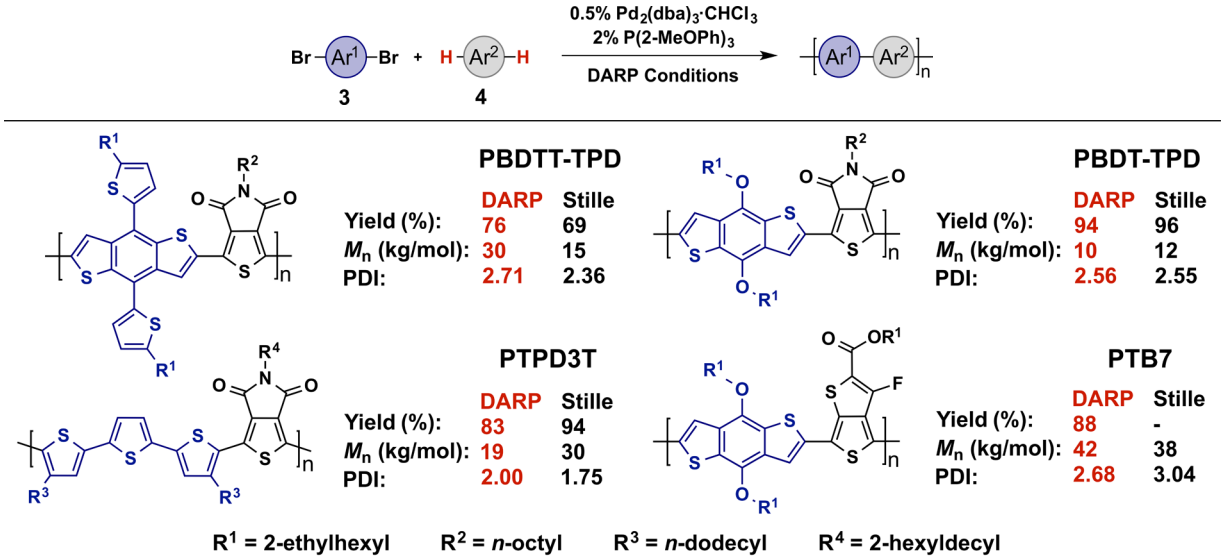

[a]DARP reaction conditions: comonomer $\mathbf{Ar^1Br_2}$ (0.1 mmol), comonomer $\mathbf{Ar^2H_2}$ (0.1 mmol), $Pd_2(dba)_3{\cdot}CHCl_3$ (0.5 mol%), P(2-MeOPh)$_3$ (2 mol %), Cs_2CO_3 (3 equiv), and 2,2-diethylhexanoic acid (DEHA) (25 mol%) in 2.00 mL of 2-methyltetrahydrofuran at 85 °C for 24 h. Yields are isolated yields after purification via Soxhlet extraction. M_ns are determined by GPC at 150 °C in 1,2,4-trichlorobenzene. Full details of Stille synthesis available in SI. DARP **PTPD3T** prepared with pivalic acid (25 mol%) in place of DEHA.

suggesting that solubility may then limit further chain elongation since the reaction mixture gels at both 50 and 75 mM. Phosphine ligand effects were also explored and tris(2-methoxyphenyl)phosphine was by far the most efficient, affording **PBDTT-FTTE** in highest yield and M_n (Table S7 in SI). Notably, tri(*o*-tolyl)phosphine and tris(4-methoxyphenyl)phosphine fail to yield any copolymer, underlining the crucial role of the coordinating *ortho*-methoxy ligand groups, as demonstrated by Ozawa.[73,74,79,80] However, using other triaryl and dialkylbiaryl phosphines having proximal coordinating groups also results in significantly lower M_ns and yields (Table S7 in SI). Finally, the DARP reaction conditions producing batch 2 were repeated two additional times affording **PBDTT-FTTE** batches in high yields (≥95%) and with similar M_ns and optical absorbance properties evidencing the high

DOI: 10.1021/jacs.6b10023
J. Am. Chem. Soc. 2016, 138, 15699−15709

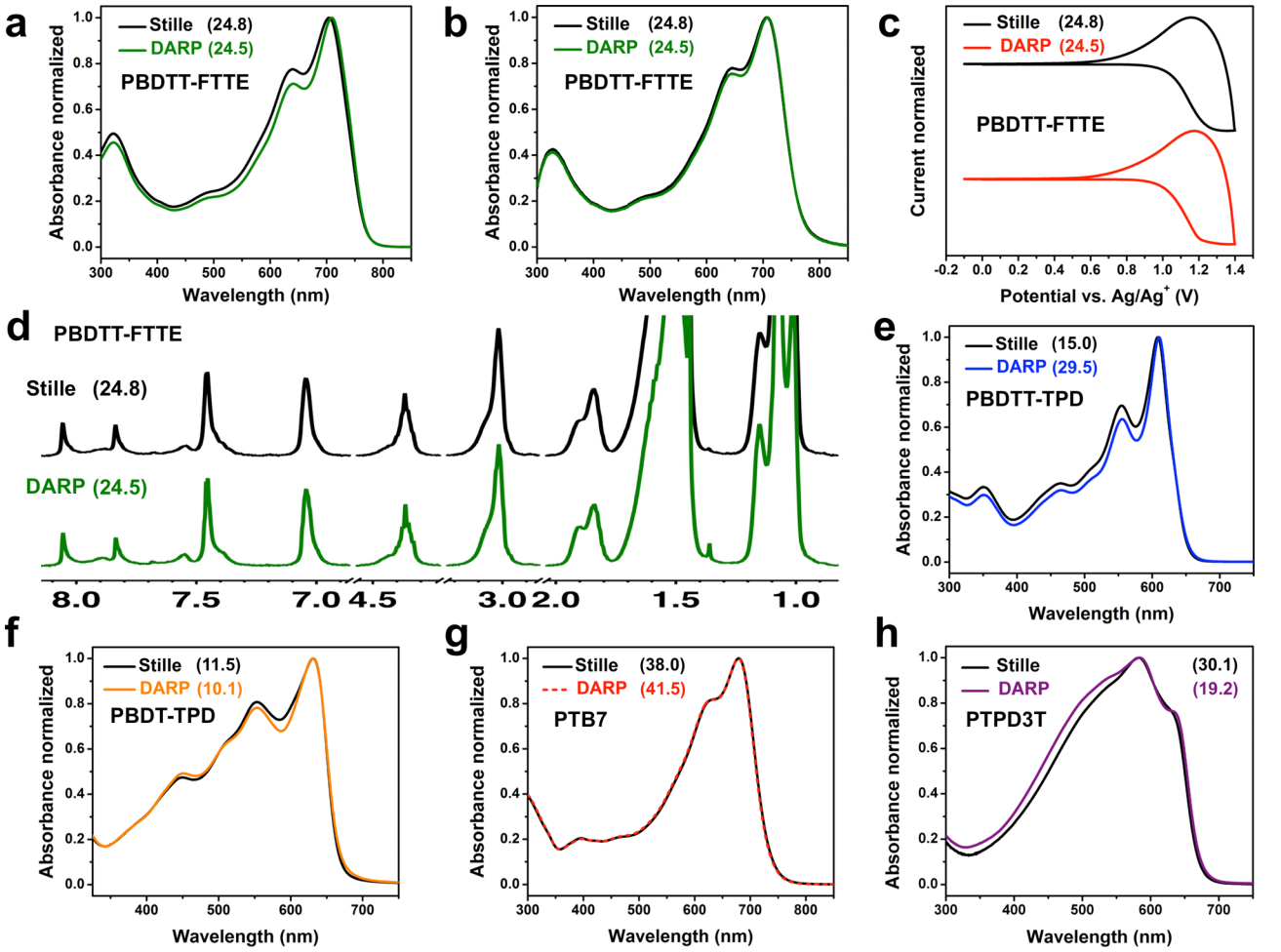

Figure 2. Comparison of DARP and Stille copolymers by optical spectroscopy, cyclic voltammetry, and NMR spectroscopy. UV−vis absorption spectra of Stille and DARP **PBDTT-FTTE** in dilute 1,2-dichlorobenzene solutions (0.013 mg/mL) (a) and in thin films spun-cast from 1,2-dichlorobenzene (b), displaying very similar absorption features. Plots are normalized to absorbance maxima. (c) Cyclic voltammograms of Stille and DARP **PBDTT-FTTE** thin films. (d) Expansion of high-temperature solution phase ^{1}H NMR stack spectra of Stille and DARP **PBDTT-FTTE** in $C_2D_2Cl_4$ at 120 °C, indicating great chemical similarity. Solution UV−vis absorption spectra of Stille and DARP **PBDTT-TPD** in $CHCl_3$ (0.013 mg/mL) (e), **PBDT-TPD** in chlorobenzene (0.013 mg/mL) (f), **PTB7** in chlorobenzene (0.013 mg/mL) (g), and **PTPD3T** in $CHCl_3$ (0.015 mg/mL) (h). Analogous features and matching or better relative absorption band intensities imply similar regularity between Stille and DARP copolymers. Numbers in parentheses correspond to copolymer number-average molecular weights (M_ns).

reproducibility of this method (Table S11 and Figure S12 in SI).

The **PBDTT-FTTE** produced under optimized DARP conditions (batch 2) compares favorably with batches synthesized using literature DARP protocols (Table 1, batches 5−8) that previously afforded copolymers with high PCEs. Specifically, the reaction conditions for batches 5,[35] 6,[36] and 7[37] produce **PBDTT-FTTE** in low yields and M_ns. The optical spectra of these copolymers do not exhibit peak maxima or vibronic structure similar to the Stille copolymer (Figure S10 in SI), reflecting the low M_ns (<6 kg/mol) and/or polymerization defects.[22,26,29] Somewhat more encouraging results are obtained under batch 8 reaction conditions,[38] which provide moderate M_n = 16 kg/mol and optical absorption features similar to the Stille copolymer (Table S9 and Figure S10 in SI). Note however that this copolymer does not exhibit the same degree of solution aggregation as the Stille sample, and using 10% Pd catalyst is not as cost-effective.[8,12] It will also be seen below that these batches exhibit lower PSC performance versus the optimized DARP- and Stille-derived samples (Table S10 in SI). Overall, we have identified reaction conditions, which provide copolymers with respectable M_ns and minimal structural defects, through careful tuning of catalytic system components and reaction parameters that feature an environmentally friendly solvent and a new sterically demanding carboxylic acid additive.

Polymerization Scope. Having in hand a set of optimized conditions, we explored the generality of this new DARP method. Four additional copolymer targets, poly{4,8-bis(2-ethylhexyloxy)-benzo[1,2-*b*:4,5-*b*′]dithiophene-2,6-diyl-*alt*-5-octyl-4*H*-thieno[3,4-*c*]pyrrole-4,6(5*H*)-dione-1,3-diyl} (**PBDT-TPD**),[28,81−84] poly{4,8-bis(2-ethylhexyloxy)benzo[1,2-*b*:4,5-*b*′]dithiophene-2,6-diyl-*alt*-(4-(2-ethylhexyl)-3-fluorothieno-[3,4-*b*]thiophene-2-carboxylate-2,6-diyl)} (**PTB7**),[85−88] poly-[5-(2-hexyldodecyl)-4*H*-thieno[3,4-*c*]pyrrole-4,6(5*H*)-dione-1,3-yl-*alt*-4,4″-dodecyl-2,2′:5′,2″-terthiophene-5,5″-diyl] (**PTPD3T**),[29,89,90] and poly{4,8-bis(5-(2-ethylhexyl)thiophen-2-yl)benzo[1,2-*b*:4,5-*b*′]dithiophene-*alt*-5-octyl-4*H*-thieno[3,4-*c*]pyrrole-4,6(5*H*)-dione} (**PBDTT-TPD**),[91,92] all having known high PCEs, and **PBDTT-TPD** with a high open-circuit voltage (V_{oc}) ∼1.0 V, were synthesized (Table 2). For comparison, these copolymers were also prepared using

DOI: 10.1021/jacs.6b10023
J. Am. Chem. Soc. 2016, 138, 15699−15709

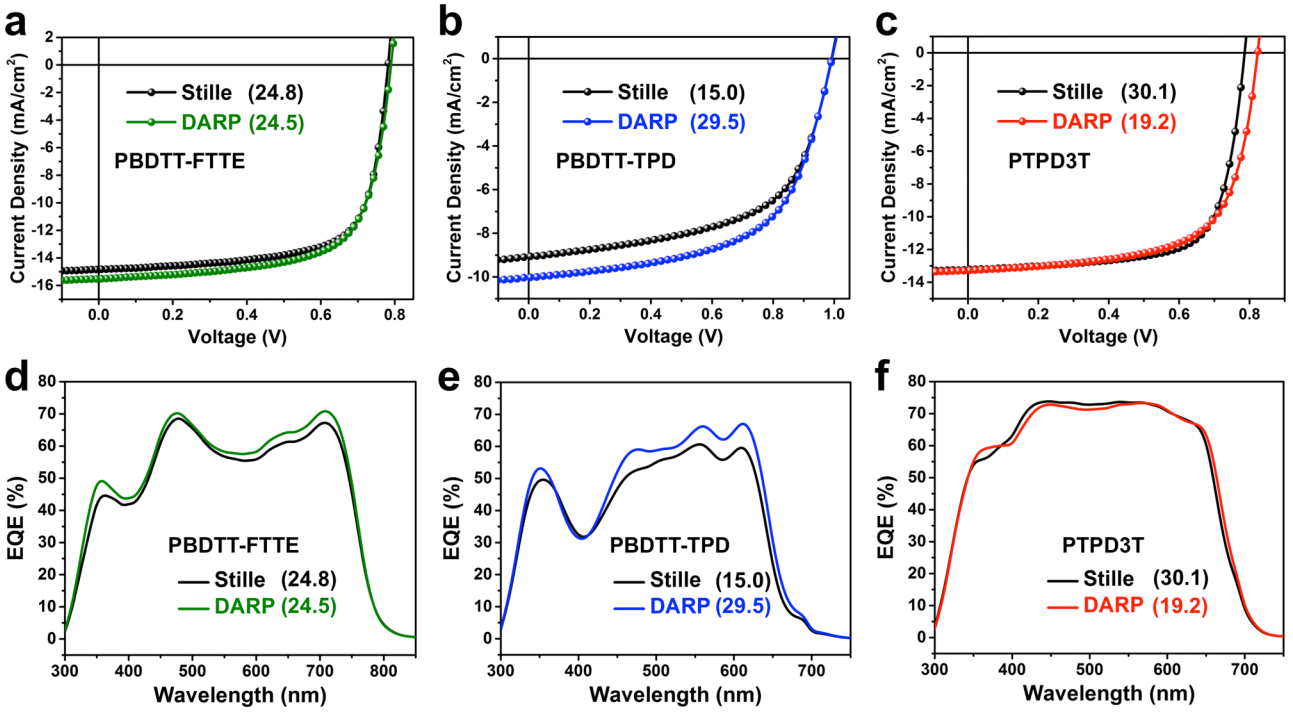

Figure 3. Comparison of the photovoltaic performance of the DARP and Stille copolymers. (a–c) Current–voltage characteristics of champion PSCs using **PBDTT-FTTE:$PC_{71}BM$** (a), **PBDTT-TPD:$PC_{61}BM$** (b), and **PTPD3T:$PC_{71}BM$** (c) blends under simulated AM 1.5 G illumination at 100 mW cm^{-2}. (d–f) External quantum efficiency (EQE) spectra for the corresponding devices. Numbers in parentheses correspond to copolymer number-average molecular weights (M_ns).

traditional Stille polycondensation following reported procedures that led to high PCE copolymers (see Section 3 in SI). The DARP copolymers are obtained in high yields, with similar dispersities, and with M_ns rivalling or exceeding those of the reference Stille-derived samples. For **PTPD3T** polymerization, the DEHA additive was replaced with smaller PivOH to accelerate the reactivity since the dihalogenated terthiophene comonomer is already sterically congested with β-alkyl substituents.[52] Finally, the DARP copolymer **PBDTT-TPD** was synthesized at both a 0.1 and 0.5 mmol comonomer scale to investigate the scalability of the DARP process and both copolymers were isolated in good yields and with similar M_ns, dispersities, and optical absorption properties (Table S12 and Figure S13 in SI).

Copolymer Characterization. The optical properties of thin films and solutions of the DARP and Stille copolymers from Table 2 as well as **PBDTT-FTTE** batches 1 and 2 are summarized in Figure 2 and Table S13 in SI. Absorption features of the DARP **PBDTT-FTTE** (Table 1, batch 2) show remarkable similarity to those of the reference Stille copolymer (Figure 2a,b). As thin films, the two samples exhibit λ_{max} at 707–708 nm and a secondary absorption maximum/shoulder at 645 nm. In both solution and film, the DARP copolymer exhibits a greater degree of aggregate ordering than the Stille copolymer (Figure 2a,b; Table 1), as judged from the $A_{0\text{-}0}/A_{0\text{-}1}$ ratios. The $A_{0\text{-}0}/A_{0\text{-}1}$ ratio is known to depend on properties such as M_n, dispersity, regioregularity, structural defects, and crystallinity.[27,28,75,77,93,94] Considering the very close M_ns and dispersities of the DARP and Stille copolymers (Table 1, batches 1 and 2), this observation suggests that there is likely greater structural order in DARP-derived **PBDTT-FTTE**. The optical band gaps (E_g^{opt}) of the DARP and Stille batches were calculated from the film absorption onsets and found to be identical, 1.62 eV. The cyclic voltammetry (CV)-derived highest occupied molecular orbital (HOMO) energies of the DARP and Stille **PBDTT-FTTE** are −5.44 and −5.46 eV, respectively, and the nearly identical cyclic voltammogram shapes imply very similar redox properties (Figure 2c). High-temperature solution phase ^1H and ^{19}F NMR spectroscopy of the DARP and Stille **PBDTT-FTTE** samples (Figure 2d and SI) exhibit no discernible differences in peak shapes or relative intensities, and no evidence of copolymer branching or other structural defects. Broad peaks in the aromatic region are attributed to copolymer aggregation and can be reduced in intensity through copolymer sample dilution (see SI).

The DARP- and Stille-derived **PBDTT-TPD**, **PBDT-TPD**, **PTB7**, and **PTPD3T** samples also exhibit significant structural similarity. The solution optical spectra are directly compared in Figure 2e–h. Again, the similarity in absorption features is particularly striking, evident from the perfectly matching lineshapes and in some cases, greater $A_{0\text{-}0}/A_{0\text{-}1}$ ratios for the DARP copolymers. The slightly broader solution optical spectrum of DARP **PTPD3T** is consistent with its slightly lower M_n relative to the Stille sample.[29] Furthermore, these DARP and Stille samples display very similar ^1H NMR spectra, cyclic voltammograms, and optical bandgaps (see Section 6 in SI). Collectively, these data indicate that the present DARP conditions furnish π-conjugated donor–acceptor copolymers that are chemically very similar to, if not more regular than, those prepared via traditional tin-based Stille polycondensation.

Solar Cell Performance. The utility of the present DARP method would only be valid if it produced copolymers with PSC performance rivalling or exceeding that of the corresponding Stille-derived copolymers. Consequently, PSCs were fabricated with the inverted cell architecture, ITO/ZnO/copolymer:$PC_{71}BM$/MoO_3/Ag, for **PBDTT-FTTE** and

DOI: 10.1021/jacs.6b10023
J. Am. Chem. Soc. 2016, 138, 15699–15709

Table 3. Photovoltaic Parameters for Solar Cells Based on DARP and Stille Copolymers[a]

copolymer	batch	V_{oc} (V)	J_{sc} (mA cm^{-2})	FF (%)	PCE (%)
PBDTT-FTTE	Stille	0.78 (0.78)	15.0 (14.9)	70.2 (72.2)	8.24 (8.40)
	DARP	0.77 (0.78)	15.5 (15.5)	68.3 (68.8)	8.19 (8.36)
PBDTT-TPD	Stille	0.99 (0.99)	8.9 (9.1)	57.8 (57.9)	5.10 (5.20)
	DARP	0.99 (0.99)	10.0 (10.0)	57.8 (58.7)	5.71 (5.84)
PTPD3T	Stille	0.79 (0.78)	13.0 (13.2)	70.4 (71.1)	7.20 (7.38)
	DARP	0.81 (0.82)	12.9 (13.3)	65.8 (66.0)	6.86 (7.20)

[a]Performance metrics are averages of 8−39 devices of each type. Values in parentheses are for champion cells. For complete statistical data see Table S15, Figures S17 and S18 in SI.

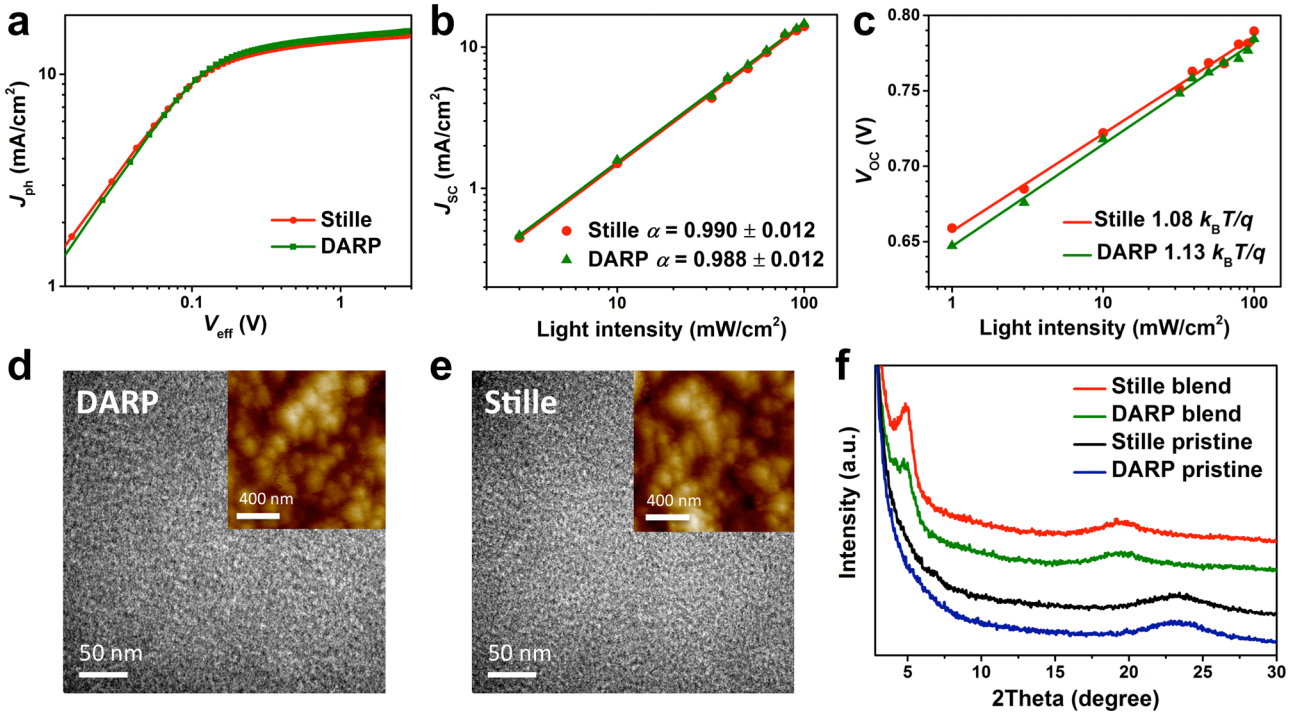

Figure 4. Comparison of DARP and Stille **PBDTT-FTTE** blend photophysical and morphological properties. (a) Photocurrent density (J_{ph}) plotted with respect to effective voltage (V_{eff}). (b) Dependence of J_{sc} on incident light intensity for DARP and Stille **PBDTT-FTTE:PC$_{71}$BM** solar cells. (c) Dependence of V_{oc} on incident light intensity. TEM images of optimized DARP (d) and Stille (e) **PBDTT-FTTE:PC$_{71}$BM** blend films. Insets: Corresponding tapping-mode AFM topographical images. (f) 2Θ XRD scattering patterns from DARP and Stille **PBDTT-FTTE** pristine films and optimized **PBDTT-FTTE:PC$_{71}$BM** blend films spin-coated on Si/SiO$_2$/ZnO substrates.

PTPD3T, and with conventional cell architecture, ITO/poly(3,4-ethylenedioxythiophene):poly(styrenesulfonate) (PEDOT:PSS)/copolymer:PC$_{61}$BM/LiF/Al, for **PBDTT-TPD**, using DARP or Stille copolymers in the photoactive layer, and their performance was evaluated (see SI for complete PSC fabrication details). Furthermore, the PSC performances of DARP **PBDTT-FTTE** batches synthesized during the optimization studies (*vide supra*) were also evaluated, and the data for these lower performing samples are summarized in Tables S2, S4, S6, and S8 in SI. Figure 3a−c shows representative current density−voltage (J−V) characteristics, and Figure 3d−f shows the external quantum efficiency (EQE) spectra of the optimized PSCs; photovoltaic performance parameters are compiled in Table 3 and Table S15 in SI.

Note that the DARP and Stille devices exhibit remarkably similar photovoltaic performance with DARP-derived **PBDTT-TPD** actually outperforming its Stille counterpart in PCE (Table 3). Comparison of the photovoltaic data in Table 3 reveals close congruence in open-circuit voltage (V_{oc}) values between the Stille- and DARP-derived **PBDTT-FTTE**, **PBDTT-TPD**, and **PTPD3T** copolymer samples, implying essentially identical frontier molecular orbital (FMO) energies and electronic delocalization, consistent with the measured similarity in HOMO energies (Table S14 in SI).[1] Very similar short-circuit current density (J_{sc}) and fill factor (FF) values are found for the DARP and Stille **PBDTT-FTTE**-based PSCs, yielding indistinguishable PCEs (Figure S17 in SI). Note that a higher J_{sc}, and a consequently higher PCE, is obtained for the DARP **PBDTT-TPD** relative to the Stille copolymer, consistent with the greater DARP sample M_n.[28,30,31] PSCs fabricated with either Stille or DARP **PTPD3T** exhibit identical J_{sc} values of ∼13.0 mA/cm^2. The lower FF for the DARP **PTPD3T**-based PSCs yields slightly lower PCEs, which nonetheless still attain >95% of the Stille performance and would set a PCE record for DARP-based PSCs if not for the present **PBDTT-FTTE** results. Furthermore, within each copolymer series the DARP and Stille PSC EQE spectra reveal very similar photoresponses (Figure 3d−f), with minor

DOI: 10.1021/jacs.6b10023
J. Am. Chem. Soc. 2016, 138, 15699−15709

variations correlating directly with the aforementioned J_{sc} differences. These results clearly demonstrate close photovoltaic similarities between the present optimized DARP copolymers and the Stille reference samples (Table S15, Figures S17 and S18 in SI).

In regard to materials prepared by literature DARP protocols, note that the PCEs of **PBDTT-FTTE** batches 5−8 lie far below those of the Stille copolymer, delivering 1.9% to 4.9% average PCEs−markedly below the ∼8.2% PCEs for optimized DARP and Stille **PBDTT-FTTE:PC$_{71}$BM** cells (Table S10 in SI). Representative J−V plots, EQE spectra, and photovoltaic metrics are collected in Figure S11 and Table S10 in SI. The observed PCE losses primarily reflect lower J_{sc} and FF values, in accord with the lower M_ns, and suggest potential structural defects.[27,28,39] Not surprisingly, the batch 5−7 EQE spectra evidence decreased photoresponse over the entire wavelength range (Figure S11 in SI). Furthermore, variation in V_{oc} up to 60 mV versus reference Stille PSCs indicates dissimilar copolymer FMO energetics.[1] Together these data support the superiority of the present DARP approach to producing high-performance photovoltaic copolymers.

Comparative PBDTT-FTTE:PC$_{71}$BM Charge Transport, Generation, and Recombination Dynamics. Thin-film charge transport perpendicular to the substrate was evaluated using a space-charge limited current (SCLC) model.[95] SCLC hole mobilities of the optimized DARP and Stille **PBDTT-FTTE:PC$_{71}$BM** thin films were measured in hole-only diodes of architecture, ITO/PEDOT:PSS/PBDTT-FTTE:PC$_{71}$BM/MoO_3/Au. Average DARP and Stille blend mobilities are comparable, $(1.7 \pm 0.3) \times 10^{-6}$ and $(1.2 \pm 0.2) \times 10^{-6}$ cm^2 V^{-1} s^{-1}, respectively (Figure S19 in SI), with minor differences correlating with the increased degree of copolymer aggregation (Figure 2a,b) and in accord with the slightly higher J_{sc} values of the DARP-based PSCs.[31,70] These data support a low defect density in the DARP films.[39]

Photocurrent density (J_{ph}) versus effective applied voltage (V_{eff}) measurements were next performed on optimized DARP and Stille **PBDTT-FTTE:PC$_{71}$BM** PSCs to compare respective charge generation processes,[70] and representative plots are provided in Figure 4a. Here $J_{ph} = J_L - J_D$, where J_L and J_D are the current densities under 1.0 sun illumination and in the dark, respectively, and $V_{eff} = V_0 - V_a$, where V_0 is the voltage at which $J_{ph} = 0$ and V_a is the applied bias. The J_{ph} values of the DARP and Stille devices reach comparable average saturation current densities (J_{sat}) of 15.8 mA cm^{-2} (16.2 mA cm^{-2} maximum) and 15.2 mA cm^{-2} (15.6 mA cm^{-2} maximum), respectively, at high biases ($V_{eff} > 2.5$ V). Under high V_{eff} conditions, all photogenerated excitons are expected to dissociate into free charge carriers, and J_{sat} can be expressed as $J_{sat} = qLG_{max}$, where G_{max} is the maximum exciton generation rate, q is the elementary charge, and L is the active layer thickness.[70] The average G_{max} values for the DARP and Stille devices are similar at $(1.10 \pm 0.05) \times 10^{28}$ and $(1.05 \pm 0.03) \times 10^{28}$ m^{-3} s^{-1}, respectively.[70] Marginal gains in G_{max} and J_{sat} exhibited by the best DARP devices can be explained by slightly higher active layer light absorption, consistent with the superior optical properties of the DARP copolymer, namely the higher $A_{0\text{-}0}/A_{0\text{-}1}$ ratio versus the Stille copolymer (Figure 2b). We also compared the exciton dissociation probabilities, $P(E,T)$, determined from the ratio J_{ph}/J_{sat}. The $P(E,T)$ values at the short-circuit (J_{sc}) conditions ($V_a = 0$ V) for the DARP and Stille cells are 93.2% and 94.2%, respectively, indicating very similar free charge generation efficiencies.[70] These results are in excellent agreement with the observed, nearly identical, FMO energies for the two copolymer batches and similar copolymer blend thin film morphologies (*vide infra*).

Finally, insights into the relative charge recombination dynamics of the two PSCs are obtained from light intensity dependent J−V measurements.[70] The dependence of PSC J_{sc} on incident light intensity can be described by $J_{sc} \propto (I_{light})^{\alpha}$, where I_{light} is incident light intensity and α is an exponential factor related to device recombination losses. $\alpha = 1$ indicates weak or no bimolecular recombination, while $\alpha < 1$ implicates bimolecular recombination losses.[96,97] Here, both the DARP and Stille devices exhibit a linear dependence of $\log(J_{sc})$ on $\log(I_{light})$ and yield almost identical exponential factors (Figure 4b). The extracted α values for the DARP and Stille cells are 0.988 ± 0.012 and 0.990 ± 0.012, respectively, similar to previously reported values for **PBDTT-FTTE:PC$_{71}$BM** cells and corresponding to very weak bimolecular recombination in both devices.[70] Figure 4c illustrates the PSC V_{oc} dependence on incident light intensity. A plot of V_{oc} versus $\ln(I_{light})$ exhibits a linear dependence with a slope of nk_BT/q, where k_B is Boltzmann's constant, T is the temperature, q is the elementary charge, and n is an ideality factor.[98] The value of the ideality factor can indicate the type of recombination in a solar cell, $n = 1$ corresponding to purely bimolecular and $n = 2$ indicating purely trap-assisted (Shockley−Read−Hall) recombination, while intermediate values ($1 < n < 2$) are consistent with the presence of both bimolecular and trap-assisted processes.[70,99] The observed ideality factors for the DARP and Stille cells are found to be 1.13 ± 0.08 and 1.08 ± 0.06, respectively,[33] implying almost identical recombination processes with only minor trap-assisted losses occurring in both PSCs. Therefore, DARP-derived **PBDTT-FTTE** does not contain excess structural defects which would create trapping centers and higher recombination losses relative to the Stille-derived copolymer.[39]

Film Morphology. The morphological properties of the DARP and Stille **PBDTT-FTTE** films were compared using AFM, TEM, and XRD techniques. Optimized **PBDTT-FTTE:PC$_{71}$BM** blend film surface morphology was investigated by tapping-mode AFM, and images are shown in Figure 4d,e insets (see also Figure S20 in SI). The blend films exhibit very similar morphological properties with relatively homogeneous surfaces and comparable aggregation feature sizes. Accordingly, the rms surface roughness of the DARP and Stille blend films are 1.39 and 1.21 nm, respectively, in accord with the literature data.[55] Top-down TEM images of the DARP and Stille blend films (Figure 4d,e) reveal uniform nanoscale phase-separation that is indistinguishable between the samples (Figure S21 in SI). No large-scale phase separation or ordered nanostructures are observed, consistent with the amorphous nature of **PBDTT-FTTE** copolymer films.[54,55]

XRD measurements on pristine DARP and Stille **PBDTT-FTTE** samples as well as on the corresponding PC$_{71}$BM blends were next performed to probe film microstructure. Crystallographic parameters are summarized in Table S16 in SI. Thin films of pristine and blended **PBDTT-FTTE** display almost identical scattering patterns (Figure 4f). In the pristine copolymer films, the absence of a reflection at $2\Theta \approx 3°$−$10°$ indicates amorphous morphology without ordered lamellar packing.[100] Both pristine films exhibit weak diffraction at $2\Theta = 22.9°$ corresponding to interchain π−π stacking (d_{010}) with a distance ∼3.88 Å.[55] Blend films of DARP and Stille **PBDTT-FTTE** with PC$_{71}$BM display a new diffraction at $2\Theta = 4.9°$ with

DOI: 10.1021/jacs.6b10023
J. Am. Chem. Soc. 2016, 138, 15699−15709

similar intensity, corresponding to lamellar (d_{100}) packing with a distance ~18 Å, attributable to $PC_{71}BM$-induced copolymer crystallization. Additionally, a shift of the $\pi-\pi$ stacking (d_{010}) diffraction peak to $2\Theta = 19.3°$ (~4.59 Å stacking distance) is observed in both blends and is assignable to copolymer backbone interchain $\pi-\pi$ stacking and/or stacked fullerenes.[101] This peak shift is likely caused by $PC_{71}BM$ intercalation into the copolymer, which disrupts $\pi-\pi$ packing.[102] Overall, the combined AFM, TEM, and XRD results argue that the bulk morphological properties of the DARP-derived **PBDTT-FTTE** copolymer are indistinguishable from those of the Stille-derived sample, corroborating similar chemical, physical, photophysical, and photovoltaic properties.

CONCLUSIONS

A general, efficient, reproducible, and sustainable direct arylation polymerization (DARP) process for synthesizing π-conjugated in-chain donor−acceptor copolymers that features an atom-efficient, economically attractive, and environmentally benign Pd-catalyzed direct C−H functionalization process is reported. This DARP approach features low catalyst loadings, an environmentally friendly solvent, and commercially available catalyst components. Importantly, the formation of photovoltaically detrimental polymerization defects is suppressed by the addition of a sterically hindered carboxylic acid. Synthetic versatility is demonstrated by the preparation of five known high-performance semiconducting copolymers. Detailed, head-to-head comparison of this new DARP and classical Stille polycondensation methods reveals that the DARP copolymers are obtained in high yields, similar dispersities, and with comparable or superior M_ns. Furthermore, the DARP copolymers exhibit optical absorption, electrochemical, and NMR spectroscopic characteristics similar or superior to those of the Stille-derived counterparts. All data suggest the absence of significant structural defects in copolymers made via the DARP process, which ultimately results in comparable or superior photovoltaic performances versus the Stille-derived references. For the first time, it is established that DARP copolymer:fullerene-derived PSCs can exceed 8% PCE. The similarity between DARP and Stille photovoltaic fullerene blends is further validated by indistinguishable bulk charge transport, charge generation/recombination processes, and thin-film microstructural properties. Overall, the present work demonstrates that this DARP methodology offers a cost-saving and waste-reducing "green chemistry" tool for the sustainable[8,12] synthesis of defect-free high-performance π-conjugated semiconducting copolymers with photovoltaic device functionality rivaling or exceeding that of Stille copolymers.

ASSOCIATED CONTENT

Supporting Information

The Supporting Information is available free of charge on the ACS Publications website at DOI: 10.1021/jacs.6b10023.

Synthesis and characterization of monomers and copolymers, UV−vis and NMR spectra, CV characterization, OPV device fabrication, SCLC, AFM, TEM, and XRD measurements (PDF)

AUTHOR INFORMATION

Corresponding Authors

*r-chang@northwestern.edu

*a-facchetti@northwestern.edu

*t-marks@northwestern.edu

ORCID

Tobin J. Marks: 0000-0001-8771-0141

Author Contributions

§A.S.D. and T.J.A. contributed equally to this work. The manuscript was written through contributions of all authors. All authors have given approval to the final version of the manuscript.

Notes

The authors declare no competing financial interest.

ACKNOWLEDGMENTS

This research was supported in part by Argonne-Northwestern Solar Energy Research (ANSER) Center, an Energy Frontier Research Center funded by the U.S. Department of Energy, Office of Science, Office of Basic Energy Sciences, under Award Number DE-SC0001059, by the U.S. Department of Energy, Office of Science, and Office of Basic Energy Sciences, under Award Number DE-FG02-08ER46536, by AFOSR grant FA9550-15-1-0044, and by the Northwestern University Materials Research Science and Engineering Center under NSF grant DMR-1121262. A.S.D. thanks the Camille and Henry Dreyfus Postdoctoral Program in Environmental Chemistry for a fellowship, and T.J.A. thanks the NSF for a predoctoral fellowship. We thank the Integrated Molecular Structure Education and Research Center (IMSERC) for characterization facilities supported by Northwestern University, National Science Foundation (NSF) under NSF CHE-1048773, Soft and Hybrid Nanotechnology Experimental (SHyNE) Resource (NSF NNCI-1542205), the State of Illinois, and International Institute for Nanotechnology (IIN). We thank Dr. F. Melkonyan (Northwestern U.) for assistance with the XRD measurements, and Dr. L. Ye and Prof. J. Hou (Institute of Chemistry, Chinese Academy of Sciences) for helpful suggestions.

REFERENCES

(1) Yu, G.; Gao, J.; Hummelen, J. C.; Wudl, F.; Heeger, A. J. *Science* **1995**, *270*, 1789.

(2) Lu, L.; Zheng, T.; Wu, Q.; Schneider, A. M.; Zhao, D.; Yu, L. *Chem. Rev.* **2015**, *115*, 12666.

(3) Bundgaard, E.; Krebs, F. C. *Sol. Energy Mater. Sol. Cells* **2007**, *91*, 954.

(4) Krebs, F. C. *Sol. Energy Mater. Sol. Cells* **2009**, *93*, 465.

(5) Darling, S. B.; You, F. *RSC Adv.* **2013**, *3*, 17633.

(6) Zhao, J.; Li, Y.; Yang, G.; Jiang, K.; Lin, H.; Ade, H.; Ma, W.; Yan, H. *Nat. Energy* **2016**, *1*, 15027.

(7) Carsten, B.; He, F.; Son, H. J.; Xu, T.; Yu, L. *Chem. Rev.* **2011**, *111*, 1493.

(8) Burke, D. J.; Lipomi, D. J. *Energy Environ. Sci.* **2013**, *6*, 2053.

(9) Osedach, T. P.; Andrew, T. L.; Bulović, V. *Energy Environ. Sci.* **2013**, *6*, 711.

(10) Morin, P.-O.; Bura, T.; Leclerc, M. *Mater. Horiz.* **2016**, *3*, 11.

(11) Okamoto, K.; Zhang, J.; Housekeeper, J. B.; Marder, S. R.; Luscombe, C. K. *Macromolecules* **2013**, *46*, 8059.

(12) Marrocchi, A.; Facchetti, A.; Lanari, D.; Petrucci, C.; Vaccaro, L. *Energy Environ. Sci.* **2016**, *9*, 763.

(13) Bura, T.; Blaskovits, J. T.; Leclerc, M. *J. Am. Chem. Soc.* **2016**, *138*, 10056.

(14) Matsidik, R.; Komber, H.; Luzio, A.; Caironi, M.; Sommer, M. *J. Am. Chem. Soc.* **2015**, *137*, 6705.

(15) Luzio, A.; Fazzi, D.; Nübling, F.; Matsidik, R.; Straub, A.; Komber, H.; Giussani, E.; Watkins, S. E.; Barbatti, M.; Thiel, W.;

Gann, E.; Thomsen, L.; McNeill, C. R.; Caironi, M.; Sommer, M. *Chem. Mater.* **2014**, *26*, 6233.
(16) Pouliot, J.-R.; Sun, B.; Leduc, M.; Najari, A.; Li, Y.; Leclerc, M. *Polym. Chem.* **2015**, *6*, 278.
(17) Broll, S.; Nübling, F.; Luzio, A.; Lentzas, D.; Komber, H.; Caironi, M.; Sommer, M. *Macromolecules* **2015**, *48*, 7481.
(18) Estrada, L. A.; Deininger, J. J.; Kamenov, G. D.; Reynolds, J. R. *ACS Macro Lett.* **2013**, *2*, 869.
(19) Mercier, L. G.; Leclerc, M. *Acc. Chem. Res.* **2013**, *46*, 1597.
(20) Gorelsky, S. I. *Coord. Chem. Rev.* **2013**, *257*, 153.
(21) Gorelsky, S. I.; Lapointe, D.; Fagnou, K. *J. Org. Chem.* **2012**, *77*, 658.
(22) Rudenko, A. E.; Thompson, B. C. *J. Polym. Sci., Part A: Polym. Chem.* **2015**, *53*, 135.
(23) Lombeck, F.; Komber, H.; Gorelsky, S. I.; Sommer, M. *ACS Macro Lett.* **2014**, *3*, 819.
(24) Hendriks, K. H.; Li, W.; Heintges, G. H. L.; van Pruissen, G. W. P.; Wienk, M. M.; Janssen, R. A. J. *J. Am. Chem. Soc.* **2014**, *136*, 11128.
(25) Tu, G.; Bilge, A.; Adamczyk, S.; Forster, M.; Heiderhoff, R.; Balk, L. J.; Mühlbacher, D.; Morana, M.; Koppe, M.; Scharber, M. C.; Choulis, S. A.; Brabec, C. J.; Scherf, U. *Macromol. Rapid Commun.* **2007**, *28*, 1781.
(26) Rudenko, A. E.; Latif, A. A.; Thompson, B. C. *Nanotechnology* **2014**, *25*, 014005.
(27) Lombeck, F.; Komber, H.; Fazzi, D.; Nava, D.; Kuhlmann, J.; Stegerer, D.; Strassel, K.; Brandt, J.; de Zerio Mendaza, A. D.; Müller, C.; Thiel, W.; Caironi, M.; Friend, R.; Sommer, M. *Adv. Energy Mater.* **2016**, 1601232.
(28) Bartelt, J. A.; Douglas, J. D.; Mateker, W. R.; El Labban, A.; Tassone, C. J.; Toney, M. F.; Fréchet, J. M. J.; Beaujuge, P. M.; McGehee, M. D. *Adv. Energy Mater.* **2014**, *4*, 1301733.
(29) Zhou, N.; Dudnik, A. S.; Li, T. I. N. G.; Manley, E. F.; Aldrich, T. J.; Guo, P.; Liao, H.-C.; Chen, Z.; Chen, L. X.; Chang, R. P. H.; Facchetti, A.; Olvera de la Cruz, M.; Marks, T. J. *J. Am. Chem. Soc.* **2016**, *138*, 1240.
(30) van Franeker, J. J.; Heintges, G. H. L.; Schaefer, C.; Portale, G.; Li, W.; Wienk, M. M.; van der Schoot, P.; Janssen, R. A. J. *J. Am. Chem. Soc.* **2015**, *137*, 11783.
(31) Li, W.; Yang, L.; Tumbleston, J. R.; Yan, L.; Ade, H.; You, W. *Adv. Mater.* **2014**, *26*, 4456.
(32) Morin, P.-O.; Bura, T.; Sun, B.; Gorelsky, S. I.; Li, Y.; Leclerc, M. *ACS Macro Lett.* **2015**, *4*, 21.
(33) He, Z.; Xiao, B.; Liu, F.; Wu, H.; Yang, Y.; Xiao, S.; Wang, C.; Russell, T. P.; Cao, Y. *Nat. Photonics* **2015**, *9*, 174.
(34) Mercier, L. G.; Aïch, B. R.; Najari, A.; Beaupré, S.; Berrouard, P.; Pron, A.; Robitaille, A.; Tao, Y.; Leclerc, M. *Polym. Chem.* **2013**, *4*, 5252.
(35) Guérette, M.; Najari, A.; Maltais, J.; Pouliot, J.-R.; Dufresne, S.; Simoneau, M.; Besner, S.; Charest, P.; Leclerc, M. *Adv. Energy Mater.* **2016**, *6*, 1502094.
(36) Najari, A.; Beaupré, S.; Allard, N.; Ouattara, M.; Pouliot, J.-R.; Charest, P.; Besner, S.; Simoneau, M.; Leclerc, M. *Adv. Energy Mater.* **2015**, *5*, 1501213.
(37) Jo, J.; Pron, A.; Berrouard, P.; Leong, W. L.; Yuen, J. D.; Moon, J. S.; Leclerc, M.; Heeger, A. J. *Adv. Energy Mater.* **2012**, *2*, 1397.
(38) Homyak, P. D.; Tinkham, J.; Lahti, P. M.; Coughlin, E. B. *Macromolecules* **2013**, *46*, 8873.
(39) Chen, S.; Lee, K. C.; Zhang, Z.-G.; Kim, D. S.; Li, Y.; Yang, C. *Macromolecules* **2016**, *49*, 527.
(40) Kuwabara, J.; Yasuda, T.; Choi, S. J.; Lu, W.; Yamazaki, K.; Kagaya, S.; Han, L.; Kanbara, T. *Adv. Funct. Mater.* **2014**, *24*, 3226.
(41) Homyak, P. D.; Liu, Y.; Ferdous, S.; Liu, F.; Russell, T. P.; Coughlin, E. B. *Chem. Mater.* **2015**, *27*, 443.
(42) Homyak, P. D.; Liu, Y.; Harris, J. D.; Liu, F.; Carter, K. R.; Russell, T. P.; Coughlin, E. B. *Macromolecules* **2016**, *49*, 3028.
(43) Kuwabara, J.; Yasuda, T.; Takase, N.; Kanbara, T. *ACS Appl. Mater. Interfaces* **2016**, *8*, 1752.
(44) Grenier, F.; Aïch, B. R.; Lai, Y.-Y.; Guérette, M.; Holmes, A. B.; Tao, Y.; Wong, W. W. H.; Leclerc, M. *Chem. Mater.* **2015**, *27*, 2137.
(45) Marzano, G.; Kotowski, D.; Babudri, F.; Musio, R.; Pellegrino, A.; Luzzati, S.; Po, R.; Farinola, G. M. *Macromolecules* **2015**, *48*, 7039.
(46) Homyak, P. D.; Liu, Y.; Liu, F.; Russel, T. P.; Coughlin, E. B. *Macromolecules* **2015**, *48*, 6978.
(47) Kuwabara, J.; Nohara, Y.; Choi, S. J.; Fujinami, Y.; Lu, W.; Yoshimura, K.; Oguma, J.; Suenobu, K.; Kanbara, T. *Polym. Chem.* **2013**, *4*, 947.
(48) Wang, D. H.; Pron, A.; Leclerc, M.; Heeger, A. J. *Adv. Funct. Mater.* **2013**, *23*, 1297.
(49) Chang, S.-W.; Waters, H.; Kettle, J.; Kuo, Z.-R.; Li, C.-H.; Yu, C.-Y.; Horie, M. *Macromol. Rapid Commun.* **2012**, *33*, 1927.
(50) Livi, F.; Gobalasingham, N. S.; Thompson, B. C.; Bundgaard, E. *J. Polym. Sci., Part A: Polym. Chem.* **2016**, *54*, 2907.
(51) Rudenko, A. E.; Thompson, B. C. *Macromolecules* **2015**, *48*, 569.
(52) Bura, T.; Morin, P.-O.; Leclerc, M. *Macromolecules* **2015**, *48*, 5614.
(53) Rudenko, A. E.; Khlyabich, P. P.; Thompson, B. C. *ACS Macro Lett.* **2014**, *3*, 387.
(54) Chang, W.-H.; Meng, L.; Dou, L.; You, J.; Chen, C.-C.; Yang, Y.; Young, E. P.; Li, G.; Yang, Y. *Macromolecules* **2015**, *48*, 562.
(55) Zhang, S.; Ye, L.; Zhao, W.; Liu, D.; Yao, H.; Hou, J. *Macromolecules* **2014**, *47*, 4653.
(56) Liu, P.; Zhang, K.; Liu, F.; Jin, Y.; Liu, S.; Russell, T. P.; Yip, H.-L.; Huang, F.; Cao, Y. *Chem. Mater.* **2014**, *26*, 3009.
(57) Cui, C.; Wong, W.-Y.; Li, Y. *Energy Environ. Sci.* **2014**, *7*, 2276.
(58) Huang, J.; Li, C.-Z.; Chueh, C.-C.; Liu, S.-Q.; Yu, J.-S.; Jen, A. K.-Y. *Adv. Energy. Mater.* **2015**, *5*, 1500406.
(59) Jung, J. W.; Jo, J. W.; Chueh, C.-C.; Liu, F.; Jo, W. H.; Russell, T. P.; Jen, A. K.-Y. *Adv. Mater.* **2015**, *27*, 3310.
(60) Hwang, Y.-J.; Courtright, B. A. E.; Ferreira, A. S.; Tolbert, S. H.; Jenekhe, S. A. *Adv. Mater.* **2015**, *27*, 4578.
(61) Hwang, Y.-J.; Li, H.; Courtright, B. A. E.; Subramaniyan, S.; Jenekhe, S. A. *Adv. Mater.* **2016**, *28*, 124.
(62) Zhong, Y.; Trinh, M. T.; Chen, R.; Purdum, G. E.; Khlyabich, P. P.; Sezen, M.; Oh, S.; Zhu, H.; Fowler, B.; Zhang, B.; Wang, W.; Nam, C.-Y.; Sfeir, M. Y.; Black, C. T.; Steigerwald, M. L.; Loo, Y.-L.; Ng, F.; Zhu, X.-Y.; Nuckolls, C. *Nat. Commun.* **2015**, *6*, 8242.
(63) Wu, Q.; Zhao, D.; Schneider, A. M.; Chen, W.; Yu, L. *J. Am. Chem. Soc.* **2016**, *138*, 7248.
(64) Hartnett, P. E.; Margulies, E. A.; Ramakrishna Matte, H. S. S.; Hersam, M. C.; Marks, T. J.; Wasielewski, M. R. *Chem. Mater.* **2016**, *28*, 3928.
(65) Lin, Y.; Zhao, F.; He, Q.; Huo, L.; Wu, Y.; Parker, T. C.; Ma, W.; Sun, Y.; Wang, C.; Zhu, D.; Heeger, A. J.; Marder, S. R.; Zhan, X. *J. Am. Chem. Soc.* **2016**, *138*, 4955.
(66) Zhou, H.; Zhang, Y.; Mai, C.-K.; Collins, S. D.; Bazan, G. C.; Nguyen, T.-Q.; Heeger, A. J. *Adv. Mater.* **2015**, *27*, 1767.
(67) Li, N.; Brabec, C. J. *Energy Environ. Sci.* **2015**, *8*, 2902.
(68) Chen, C.-C.; Chang, W.-H.; Yoshimura, K.; Ohya, K.; You, J.; Gao, J.; Hong, Z.; Yang, Y. *Adv. Mater.* **2014**, *26*, 5670.
(69) Zhang, Q.; Wan, X.; Liu, F.; Kan, B.; Li, M.; Feng, H.; Zhang, H.; Russell, T. P.; Chen, Y. *Adv. Mater.* **2016**, *28*, 7008.
(70) Lu, L.; Chen, W.; Xu, T.; Yu, L. *Nat. Commun.* **2015**, *6*, 7327.
(71) Benten, H.; Nishida, T.; Mori, D.; Xu, H.; Ohkita, H.; Ito, S. *Energy Environ. Sci.* **2016**, *9*, 135.
(72) Jung, J.; Lee, W.; Lee, C.; Ahn, H.; Kim, B. J. *Adv. Energy Mater.* **2016**, *6*, 1600504.
(73) Wakioka, M.; Kitano, Y.; Ozawa, F. *Macromolecules* **2013**, *46*, 370.
(74) Wakioka, M.; Ichihara, N.; Kitano, Y.; Ozawa, F. *Macromolecules* **2014**, *47*, 626.
(75) Kohn, P.; Huettner, S.; Komber, H.; Senkovskyy, V.; Tkachov, R.; Kiriy, A.; Friend, R. H.; Steiner, U.; Huck, W. T. S.; Sommer, J.-U.; Sommer, M. *J. Am. Chem. Soc.* **2012**, *134*, 4790.
(76) Aycock, D. F. *Org. Process Res. Dev.* **2007**, *11*, 156.
(77) Lu, L.; Zheng, T.; Xu, T.; Zhao, D.; Yu, L. *Chem. Mater.* **2015**, *27*, 537.
(78) Schiefer, D.; Komber, H.; Keheze, F. M.; Kunz, S.; Hanselmann, R.; Reiter, G.; Sommer, M. *Macromolecules* **2016**, *49*, 7230.

DOI: 10.1021/jacs.6b10023
J. Am. Chem. Soc. 2016, 138, 15699−15709

(79) Wang, Q.; Takita, R.; Kikuzaki, Y.; Ozawa, F. *J. Am. Chem. Soc.* **2010**, *132*, 11420.
(80) Wakioka, M.; Nakamura, Y.; Montgomery, M.; Ozawa, F. *Organometallics* **2015**, *34*, 198.
(81) Zou, Y.; Najari, A.; Berrouard, P.; Beaupré, S.; Aïch, B. R.; Tao, Y.; Leclerc, M. *J. Am. Chem. Soc.* **2010**, *132*, 5330.
(82) Piliego, C.; Holcombe, T. W.; Douglas, J. D.; Woo, C. H.; Beaujuge, P. M.; Fréchet, J. M. J. *J. Am. Chem. Soc.* **2010**, *132*, 7595.
(83) Hoke, E. T.; Vandewal, K.; Bartelt, J. A.; Mateker, W. R.; Douglas, J. D.; Noriega, R.; Graham, K. R.; Fréchet, J. M. J.; Salleo, A.; McGehee, M. D. *Adv. Energy. Mater.* **2013**, *3*, 220.
(84) Bartelt, J. A.; Beiley, Z. M.; Hoke, E. T.; Mateker, W. R.; Douglas, J. D.; Collins, B. A.; Tumbleston, J. R.; Graham, K. R.; Amassian, A.; Ade, H.; Fréchet, J. M. J.; Toney, M. F.; McGehee, M. D. *Adv. Energy Mater.* **2013**, *3*, 364.
(85) Liang, Y.; Xu, Z.; Xia, J.; Tsai, S.-T.; Wu, Y.; Li, G.; Ray, C.; Yu, L. *Adv. Mater.* **2010**, *22*, E135.
(86) He, Z.; Zhong, C.; Su, S.; Xu, M.; Wu, H.; Cao, Y. *Nat. Photonics* **2012**, *6*, 591.
(87) Nian, L.; Zhang, W.; Zhu, N.; Liu, L.; Xie, Z.; Wu, H.; Würthner, F.; Ma, Y. *J. Am. Chem. Soc.* **2015**, *137*, 6995.
(88) Ouyang, X.; Peng, R.; Ai, L.; Zhang, X.; Ge, Z. *Nat. Photonics* **2015**, *9*, 520.
(89) Guo, X.; Zhou, N.; Lou, S. J.; Smith, J.; Tice, D. B.; Hennek, J. W.; Ortiz, R. P.; López Navarrete, J. T.; Li, S.; Strzalka, J.; Chen, L. X.; Chang, R. P. H.; Facchetti, A.; Marks, J. *Nat. Photonics* **2013**, *7*, 825.
(90) Zhou, N.; Guo, X.; Ortiz, R. P.; Harschneck, T.; Manley, E. F.; Lou, S. J.; Hartnett, P. E.; Yu, X.; Horwitz, N. E.; Burrezo, P. M.; Aldrich, T. J.; López Navarrete, J. T.; Wasielewski, M. R.; Chen, L. X.; Chang, R. P. H.; Facchetti, A.; Marks, T. J. *J. Am. Chem. Soc.* **2015**, *137*, 12565.
(91) Yuan, J.; Zhai, Z.; Dong, H.; Li, J.; Jiang, Z.; Li, Y.; Ma, W. *Adv. Funct. Mater.* **2013**, *23*, 885.
(92) Warnan, J.; El Labban, A.; Cabanetos, C.; Hoke, E. T.; Shukla, P. K.; Risko, C.; Brédas, J.-L.; McGehee, M. D.; Beaujuge, P. M. *Chem. Mater.* **2014**, *26*, 2299.
(93) Bencheikh, F.; Duché, D.; Ruiz, C. M.; Simon, J.-J.; Escoubas, L. *J. Phys. Chem. C* **2015**, *119*, 24643.
(94) Zhong, H.; Li, C.-Z.; Carpenter, J.; Ade, H.; Jen, A. K.-Y. *J. Am. Chem. Soc.* **2015**, *137*, 7616.
(95) Murgatroyd, P. N. *J. Phys. D: Appl. Phys.* **1970**, *3*, 151.
(96) McNeill, C. R.; Halls, J. J. M.; Wilson, R.; Whiting, G. L.; Berkebile, S.; Ramsey, M. G.; Friend, R. H.; Greenham, N. C. *Adv. Funct. Mater.* **2008**, *18*, 2309.
(97) Mandoc, M. M.; Veurman, W.; Koster, L. J. A.; de Boer, B.; Blom, P. W. M. *Adv. Funct. Mater.* **2007**, *17*, 2167.
(98) Zhou, N.; Lin, H.; Lou, S. J.; Yu, X. G.; Guo, P. J.; Manley, E. F.; Loser, S.; Hartnett, P. E.; Huang, H.; Wasielewski, M. R.; Chen, L. X.; Chang, R. P. H.; Facchetti, A.; Marks, J. *Adv. Energy Mater.* **2014**, *4*, 1300785.
(99) Cowan, S. R.; Roy, A.; Heeger, A. J. *Phys. Rev. B: Condens. Matter Mater. Phys.* **2010**, *82*, 245207.
(100) Melkonyan, F. S.; Zhao, W.; Drees, M.; Eastham, N. D.; Leonardi, M. J.; Butler, M. R.; Chen, Z.; Yu, X.; Chang, R. P. H.; Ratner, M. A.; Facchetti, A.; Marks, T. J. *J. Am. Chem. Soc.* **2016**, *138*, 6944.
(101) Kim, D. H.; Mei, J.; Ayzner, A. L.; Schmidt, K.; Giri, G.; Appleton, A. L.; Toney, M. F.; Bao, Z. *Energy Environ. Sci.* **2014**, *7*, 1103.
(102) Miller, N. C.; Cho, E.; Junk, M. J. N.; Gysel, R.; Risko, C.; Kim, D.; Sweetnam, S.; Miller, C. E.; Richter, L. J.; Kline, R. J.; Heeney, M.; McCulloch, I.; Amassian, A.; Acevedo-Feliz, D.; Knox, C.; Hansen, M. R.; Dudenko, D.; Chmelka, B. F.; Toney, M. F.; Brédas, J.-L.; McGehee, M. D. *Adv. Mater.* **2012**, *24*, 6071.

DOI: 10.1021/jacs.6b10023
J. Am. Chem. Soc. 2016, 138, 15699−15709